Journal of Catalysis 283 (2011) 192–201

Contents lists available at SciVerse ScienceDirect

Journal of Catalysis

journal homepage: www.elsevier.com/locate/jcat

Ionic liquid-enhanced immobilization of biosynthesized Au nanoparticles on TS-1 toward efficient catalysts for propylene epoxidation

Mingming Du [a], Guowu Zhan [a], Xin Yang [b], Huixuan Wang [a], Wenshuang Lin [a], Yao Zhou [a], Jing Zhu [a], Ling Lin [a], Jiale Huang [a,*], Daohua Sun [a], Lishan Jia [a], Qingbiao Li [a,*]

[a] Department of Chemical and Biochemical Engineering, College of Chemistry and Chemical Engineering, National Laboratory for Green Chemical Productions of Alcohols, Ethers and Esters, Key Lab for Chemical Biology of Fujian Province, Xiamen University, Xiamen 361005, PR China
[b] College of Chemical Engineering, Huaqiao University, Xiamen 361021, PR China

ARTICLE INFO

Article history:
Received 20 July 2011
Revised 22 August 2011
Accepted 23 August 2011
Available online 25 September 2011

Keywords:
Gold
Biosynthesis
Ionic liquid
TS-1
Catalyst
Propylene epoxidation
Immobilization
Special adsorption

ABSTRACT

The direct vapor-phase epoxidation of propylene in the presence of hydrogen and oxygen was studied at a space velocity of 7000 mL h^{-1} $g_{cat.}^{-1}$ over gold catalysts with varying gold and titanium contents prepared by ionic liquid-enhanced immobilization (ILEI) method in which biosynthesized gold nanoparticles (GNPs) were immobilized onto the titanium silicalite-1 (TS-1) supports through the assistance of a small amount of 1-butyl-3-methylimidazolium tetrafluoroborate ([BMIM][BF_4]). The results showed that $[BMIM]^+$ specially adsorbed onto the support to increase its isoelectric point, leading to the enhanced immobilization. The propylene conversion of 14.6% and PO formation rate of 164.4 g_{po} K $g_{cat.}^{-1}$ h^{-1} were higher than those in any other reports, probably attributing to enhanced interaction between the GNPs and TS-1. Furthermore, the excellent activity and high selectivity of the Au/TS-1 catalysts at a relatively high reaction temperature might be attributed to the existence of residual biomolecules on the catalysts.

1. Introduction

Propylene epoxide (PO) is an important bulk chemical widely used for the production of polyether polyols, polyurethane foams, propene glycol, and propene glycol ethers [1]. PO is industrially produced using chlorohydrin and Halcon (hydroperoxide) processes [1,2]. The former process produces environmentally unfriendly chlorinated by-products, while the later process produces large quantities of coproducts such as tert-butyl alcohol and styrene, which pose economic problems when their demand is lower than that of PO. Therefore, a great deal of effort has been put into catalytic epoxidation of propylene since the late 1990s. Clerici et al. utilized titanium silicalite (TS-1) catalyst for the epoxidation of propylene in the liquid phase using hydrogen peroxide [3,4]. However, the cost of H_2O_2 is very high and also there are handling problems when operating with H_2O_2 [5].

In 1998, a significant demonstration of gas-phase propylene epoxidation was reported by Hayashi et al. [6], who discovered that Au/TiO_2 catalysts with very fine and highly dispersed gold nanoparticles (GNPs) (2.0–5.0 nm) through deposition–precipitation (DP) exhibited a high selectivity (>90%) toward PO at low propylene conversion (~1%) using mixture of propylene, oxygen, and hydrogen under ambient pressure. To date, it has been reported that the gas-phase epoxidation of propylene has been performed over GNPs supported on a number of Ti-containing materials like TiO_2, TiO_2/SiO_2, TS-1, Ti-MCM-41, Ti-MCM-48, three-dimensional Ti–Si mesoporous materials (3D-Ti–Si), Ti-HMS, and so on [7–18]. The density functional theory (DFT) of hydroperoxy (OOH) intermediates on various model titanosilicalite Ti centers explained how microstructural aspects of Ti sites affect propylene epoxidation reactivity. It also demonstrated that a well-defined tetrahedral titanium center is essential for epoxidation [19]. These works have suggested that the isolation of Ti in tetrahedral sites is a requirement for a stable and active catalyst, motivating people to focus on TS-1 as the catalyst support. Taylor et al. found that addition of carbon pearls during the preparation of TS-1 would enhance the activity and stability of the responding Au/TS-1 catalysts prepared by DP in propylene epoxidation [16]. Though the DP method to prepare Au/TS-1 catalysts for propylene epoxidation with O_2 and H_2 mixture is very effective [10,13–18], the Au capture efficiency was always very low. A study on the DP method for Au/TS-1 catalysts has shown that only 1–3 wt.% of the gold available in solution was deposited on conventional TS-1 supports at pH of 9–10 [17]. Even though deposition of gold could be significantly boosted by pretreating TS-1

* Corresponding authors. Fax: +86 592 2184822.
E-mail addresses: cola@xmu.edu.cn (J. Huang), kelqb@xmu.edu.cn (Q. Li).

0021-9517/$ - see front matter © 2011 Elsevier Inc. All rights reserved.
doi:10.1016/j.jcat.2011.08.011

supports with NH_4NO_3 aqueous solution prior to DP [15], the capture efficiency of Au was still less than 20 wt.%. The sol-immobilization (SI) technique is also an effective method for the preparation of gold catalysts [20–23]. Compared with the DP method, the SI method has advantages because 100 wt.% of the gold in solution can be immobilized on support materials. This method has been used to prepare gold catalysts for benzyl alcohol oxidation [20,22], low-temperature CO oxidation [21,23], and propylene epoxidation [24].

In recent years, room-temperature ionic liquids (ILs) have also attracted much attention due to their special properties, such as negligible vapor pressure, wide liquid temperature range, excellent chemical stability, high thermal stability, and the strong solvent power for a wide variety of organic, inorganic, and polymeric molecules. Many reactions have been carried out in ILs [25,26]. ILs are also a good media to stabilize metal NPs [27,28] and have been used to immobilize metal NPs onto solid supports to prepare supported catalysts. For example, Han and coworkers demonstrated that Pd and Ru NPs in IL 1,1,3,3-tetramethylguanidinium lactate (TMGL) immobilized onto supports, which were obtained through reducing metal precursors by H_2, resulted in highly active heterogeneous catalysts [29–31] due to the excellent synergistic effects of IL, support, and metal nanoparticles.

Although the use of such GNPs has a high potential for propylene epoxidation, CO oxidation reactions, and so on, novel, cost-effective, and ''greener'' approaches for the preparation of gold catalysts should be developed, because GNP production remains expensive and/or involves hazardous chemicals. Biosynthesis of GNPs as an emerging highlight of the intersection of nanotechnology and biotechnology has received increasing attention due to a growing need to develop environmentally benign technologies in material in the last decade [32–37]. As an alternative to chemical methods, biosynthesis methods can be used to synthesize NPs with a narrow size distribution and a desired diameter without any auxiliary surfactant or capping agent, owing to the presence of plant biomass that plays dual roles as both reductant and stabilizer [37–42]. However, the application of the biosynthesized GNPs to catalytic system has been little reported. Vilchis-Nestor et al. prepared Au(AgAu)/SiO_2–Al_2O_3 catalysts for the oxidation and hydrogenation of CO [43], and our group has attempted to prepare Au/TS-1 catalysts for propylene epoxidation by bio-reduction synthesis method [44,45]. As mentioned above, the combination of biosynthesis and ILs may provide a new way to prepare highly efficient Au catalysts. In the present work, we report an ionic liquid-enhanced immobilization (ILEI) method to prepare the Au/TS-1 catalysts for the epoxidation of propylene. In this method, biosynthesized GNPs were immobilized onto TS-1 by IL 1-butyl-3-methylimidazolium tetrafluoroborate ([BMIM][BF_4]) from their solution. The Au/TS-1 catalysts showed an excellent performance for the vapor-phase propylene epoxidation in the presence of hydrogen and oxygen. Therefore, the ILEI method was effective for preparation of the Au/TS-1 catalysts. The method was totally different from the IL immobilization method previously reported [29–31]. In this work, the role of [BMIM][BF_4] in the ILEI method for the Au/TS-1 catalysts was investigated in detail. To the best of our knowledge, this is the first report on enhanced immobilization of biosynthesized GNPs onto solid support using IL, which will be a breakthrough for the fabrication of supported Au catalysts.

2. Experimental

2.1. Materials

C. platycladi, purchased from Xiamen Jiuding Drugstore, China, was first milled and screened by a 20-mesh sieve for further experiments. The IL, [BMIM][BF_4] (99%), was purchased from Shanghai Cheng Jie Chemical, Co. Ltd. Other chemical reagents mentioned were purchased from Sinopharm Chemical Reagent Co. Ltd., China, and were used as received.

2.2. Synthesis of TS-1 supports

TS-1 supports were synthesized using the method developed by Khomane et al. [46]. In a typical synthesis, 12.7 mL of a 40 wt.% tetrapropylammonium hydroxide (TPAOH) solution and 2 g of polyoxyethylene 20-sorbitan monolaurate (Tween 20) were dissolved in 35 mL deionized (DI) water. This solution was added dropwise to 24.6 mL of tetraethylorthosilicate (TEOS) in a polypropylene Erlenmeyer flask with vigorous stirring for 1 h. Then, 1.1 mL of titanium(IV) butoxide (TBOT) was dissolved in 6.2 mL of isopropanol under stirring. The solution was then added to the TEOS mixture dropwise during vigorous stirring. Finally, another 4.6 mL of TPAOH solution was added dropwise to the mixture under vigorous stirring, leading to a molar composition of 1.000 Si:0.029 Ti:0.300 TPAOH for the resulting synthesis solution. Afterward, the mixture was stirred for 1 h and then the mixture was transferred to a sealed Teflon-lined pressure vessel and heated at 170 °C for 24 h to facilitate the crystallization process. Next, the solid was collected via centrifugation which after being washed thoroughly with DI water, was dried in vacuum at 320 K for 24 h, and finally calcined at 550 °C for 5 h. The TS-1 support with a Si/Ti ratio of 35 was labeled as TS-1(35). Other TS-1(x) supports with different Si/Ti ratios were synthesized in the same manner.

2.3. Preparation of Au/TS-1 catalysts

The gold sol was prepared by the biosynthetic method employing plant biomass extract. In order to obtain *C. platycladi* extract, the carefully weighted biomass, 4.0 g, was added to 400 mL DI water in a conical flask of 500 mL capacity. The mixture was thereafter shaken at a rotation rate of 150 rpm for 2 h at 30 °C and filtrated to get filtrate for further experiments. In a typical synthesis of GNPs, an appropriate amount of aqueous $HAuCl_4$ solution (48.56 mM) was added to 25 mL extract in a conical flask to have a final concentration of Au(III) 0.5 mM, and the mixture was then vigorously stirred for 1 h at room temperature. It should be noted that the solution turned reddish-pink in a few seconds after $HAuCl_4$ was added into the extract, indicating fast reduction of Au^{3+} ions [37]. Afterward, 0.5 g TS-1 and 0.1 mL [BMIM][BF_4] were added to the gold sols under vigorous stirring. After 1 h, the suspension was filtered through a cellulose filter membrane with the size of pores 0.45-mm, and the retained solid was washed three times with DI water. Finally, the obtained solid, after being dried at 50 °C in vacuum for 24 h, was calcinated at 375 °C for 6 h. Thus, the obtained Au catalysts were denoted as zAu/TS-1(x)-IL, where z was the calculated weight percent of Au in the catalysts. The reference catalyst 0.5Au/TS-1(35) was synthesized in the same manner without [BMIM][BF_4], and the catalyst 0.5Au/TS-1(35)-pH was prepared through acidifying the colloid solution at pH 2 by sulfuric acid.

2.4. Characterization of the catalysts

Surface area of the TS-1 supports was measured in a Micromeritics Tristar system (Tristar 3000). Before measurements, samples were outgassed at 300 °C for 3 h. X-ray diffraction (XRD) measurement was taken on an X'Pert Pro X-ray Diffractometer (PANalytical BV, The Netherlands) operated at a voltage of 40 kV and a current of 30 mA with Cu Kα radiation. The diffuse reflectance ultraviolet–visible (DRUV–vis) spectra of the support were taken on a Varian Cary-5000 spectrometer equipped with a diffuse-reflectance accessory, using dehydrated $BaSO_4$ as a reference in the range of 200–800 nm. UV–vis spectroscopy analyses of the liquid samples

were carried out at room temperature on an UNICAM UV-300 spectrophotometer (Thermo Spectronic) from 330 to 800 nm. FTIR spectra were recorded on a Nicolet Avatar 660, where the samples were ground with KBr and pressed into thin wafer. Transmission electron microscopy (TEM) images of the samples were obtained on a Tecnai F30 microscope. Size distribution of the resulting NPs was estimated on the basis of TEM micrographs with the assistance of SigmaScan Pro software (SPSS Inc., Version 4.01.003). The actual Au loadings of the samples were determined by atomic absorption spectroscopy (AAS). And the catalysts were characterized by X-ray photoelectron spectroscopy (XPS) using a PHI Quantum-2000 spectrometer equipped with a hemispherical electron analyzer and a Al Kα (1486.6 eV) X-ray source. Zeta Plus for zeta potential analysis was from Brookhaven Instruments Corporation. TG studies were carried out on a Netzsch TG209F1 thermobalance under flowing air atmosphere at a heating rate of 10 °C min^{-1}.

2.5. Catalytic activity measurements

The catalytic tests were carried out in a half-inch-diameter vertical fixed-bed stainless steel reactor using a feed concentration of 10/10/10/70 vol.% of propylene (99.999%), O_2 (99.999%), H_2 (99.999%), and N_2 (99.999%) and 150 mg of catalyst at a space velocity of 7000 mL h^{-1} $g_{cat.}^{-1}$. The temperature was measured by using a glass tube covered Cr–Al thermocouple located in the center of the catalyst bed. The gas leaving the reactor was heated at about 100 °C and analyzed online by two gas chromatographs. One of the chromatograph was equipped with two thermal conductivity detectors (TCD), using a MS 5A packed column (2 mm × 3 m) and a Porapak Q packed column (2 mm × 3 m), respectively, and the other equipped with a flame ionization detector (FID) was attached to a Porapak T packed column (2 mm × 2 m). The MS 5A and Porapak Q columns were used to detect hydrocarbons (e.g., propylene), H_2, O_2, CO_2, N_2, and H_2O. The Porapak T column was used to detect oxygenates (e.g., propylene, acetaldehyde, PO, acetone, propionaldehyde, acrolein, and the like).

3. Results and discussion

3.1. Characterizations of TS-1 supports

Textural properties of the prepared TS-1 supports are shown in Table 1. Little change in the surface properties with increasing titanium content in the supports indicated that Ti atoms were either well dispersed on the walls of the silica matrix or present inside the framework without pore blocking effect. XPS analysis of TS-1 indicated that surface composition was approximate to theoretical value. XRD patterns of the TS-1 supports with different Si/Ti ratios (Fig. 1) showed that all the supports are highly crystalline TS-1 with the MFI structure [47,48]. As evidenced by the disappearance of diffraction lines splitting at $2\theta = 24.5°$ and 29.5° (marked with arrows), the conversion of the monoclinic structure of silicalite-1 to an orthorhombic structure indicated the incorporation of Ti(IV) into the framework. The typical FTIR absorption spectra of the TS-1 supports (Fig. 2A) show that the absorption band at 960 cm^{-1} was observed in all the cases due to incorporation of titanium into the framework. Moreover, the absorption band at 960 cm^{-1} decreased with decreasing titanium content. The DRUV–vis spectra of the TS-1 supports (Fig. 2B) with Si/Ti = 35, 48, 100, and 200 resulted in the absorption bands around 210 nm, which were indicative of tetrahedral titanium species substitution into the zeolite framework. There was no other absorption band in these samples implying no extraframework species in the silicalite-1 framework [48]. Next, the TS-1 supports were used for investigation of the ILEI method.

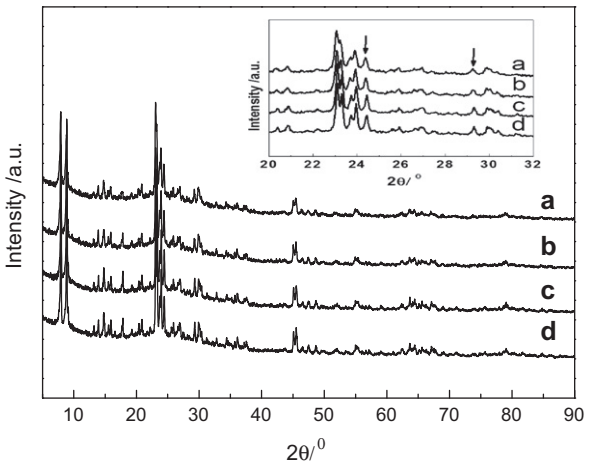

Fig. 1. XRD patterns of TS-1 supports with different Si/Ti ratios. (a) TS-1(35), (b) TS-1(48), (c) TS-1(100), and (d) TS-1(200).

3.2. Characterizations of the Au/TS-1 catalysts

The Au/TS-1-IL catalysts were prepared by immobilizing GNPs onto the TS-1 supports through the ILEI method. In this work, the GNPs were biologically synthesized by the reduction of $HAuCl_4$ with *C. platycladi* extract leading to a reddish-pink sol within a few seconds. Fig. 3A shows the typical TEM image of the GNPs synthesized by reducing aqueous $HAuCl_4$ (0.5 mM) with *C. platycladi* extract. The well-dispersed GNPs mostly ranging from 2.0 to 5.0 nm with a mean diameter of 3.1 nm (the insert image in Fig. 3A) are proper for preparation of the Au/TS-1 catalysts. The representative TEM image of Au/TS-1(35)-IL in Fig. 3B clearly illustrates that the GNPs with a mean diameter around 3.6 nm (the insert image in Fig. 3B) were well dispersed on the TS-1 surfaces. Evidently, the GNPs nearly retained their size after immobilization on TS-1 supports through the ILEI method.

FT-IR spectroscopy was employed to determine the presence of the [BMIM][BF_4] on the Au/TS-1 catalysts. The FT-IR spectrum of [BMIM][BF_4] (Fig. 4a) shows that the C–H stretching region between 2700 and 3200 cm^{-1} possessed the strongest absorption. The absorption band at 1570 cm^{-1} could be assigned to the C=N stretching vibration of IL [49]. The FT-IR spectrum of the catalyst 0.5Au/TS-1(35)-IL before being pretreated under air (Fig. 4c) shows

Table 1
Characterization of the TS-1 supports.

Sample	Normal Si/Ti	$(Si/Ti)_{xps}$	D_{TS-1} (nm)	S_{BET} (m^2 g^{-1})	Pore diameter[a] (nm)	Pore vol.[b] (cm^3 g^{-1})
TS-1(35)	35	40.6	270 ± 22	444	5.6	0.35
TS-1(48)	48	50.2	253 ± 23	474	4.7	0.35
TS-1(100)	100	111.2	244 ± 21	446	5.0	0.32
TS-1(200)	200	195.3	234 ± 26	427	4.9	0.33

[a] Calculated from the desorption branch of nitrogen isotherm by using the BJH model.
[b] Calculated from the volume adsorbed of P/P_0 at 0.99.

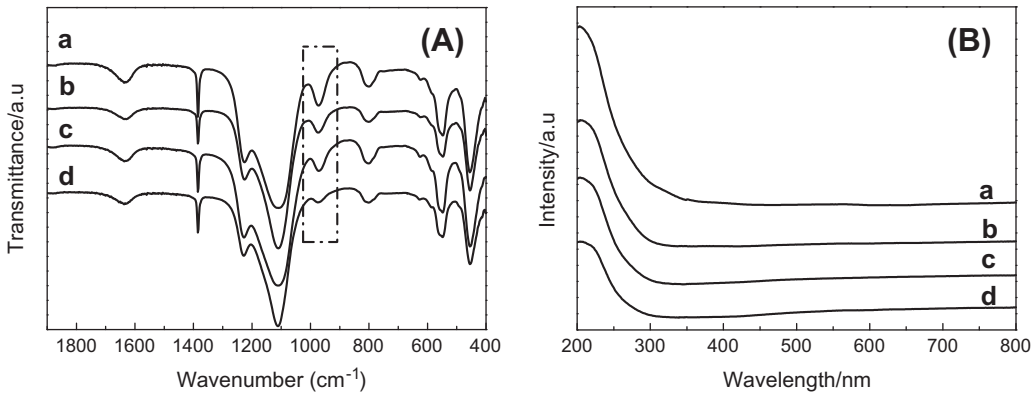

Fig. 2. FT-IR (A) and DRUV–vis (B) of TS-1 supports with different Si/Ti ratios. (a) TS-1(35), (b) TS-1(48), (c) TS-1(100), and (d) TS-1(200).

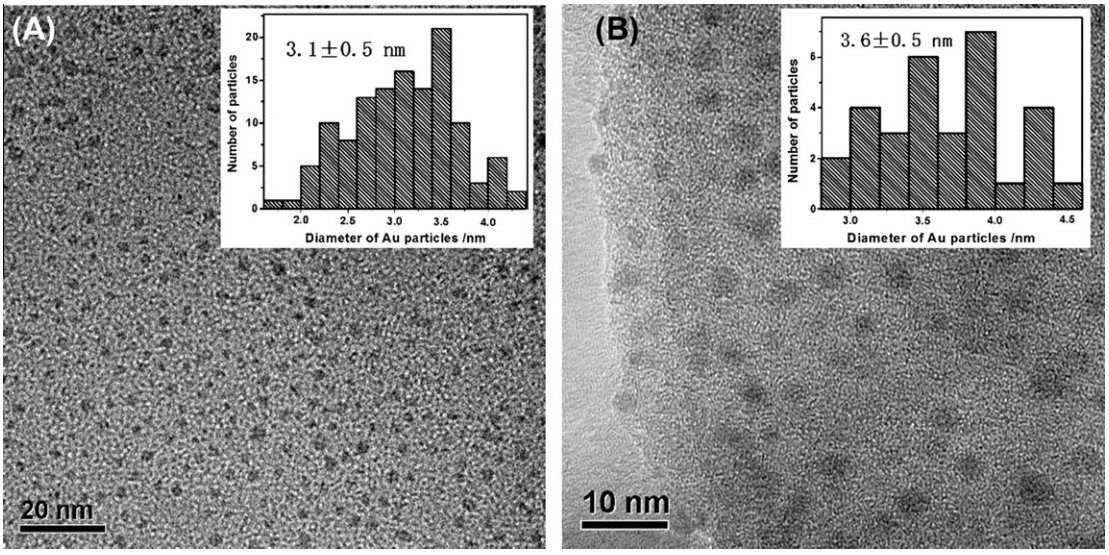

Fig. 3. TEM images and corresponding histogram of size distribution of GNPs (A) and the catalyst 0.5Au/TS-1(35)-IL (B) by *C. platycladi* extract; [$HAuCl_4$] = 0.5 mmol L^{-1}; [*C. platycladi*] = 10.0 g L^{-1}; reaction temperature is 30 °C.

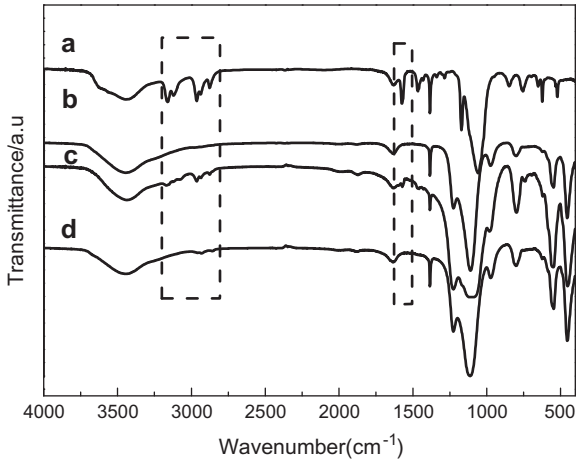

Fig. 4. FT-IR spectra of [BMIM][BF4] (a), TS-1(35) (b), 0.5Au/TS-1(35)-IL before calcination (c) and 0.5Au/TS-1(35)-IL after calcination (d).

the CH stretching region between 2700 and 3200 cm^{-1} and the absorption band of C=N stretching vibration at 1570 cm^{-1}, besides the typical absorption bands of the TS-1(Fig. 4b), suggesting that the $[BMIM]^+$ ions adsorbed on the TS-1 surface, and these adsorbed $[BMIM]^+$ ions cannot be removed by washing. No absorption bands of $[BMIM]^+$ ions were presented in the FTIR spectrum (Fig. 4d) of the catalyst after pretreatment under air at 375 °C for 6 h meaning that the IL had been decomposed.

Nitrogen physisorption measurements were also taken for the Au/TS-1 catalysts through the ILEI method with different gold loadings. The pore structure parameters, such as the specific area (S_{BET}), pore volume, and pore diameter of the TS-1 and Au/TS-1 catalysts, are summarized in Table 2. After Au immobilization, the surface area of the supports slightly decreased, while the pore diameter slightly increased, in comparison with those of the pristine TS-1 support (Table 1). The isotherms of type IV, typical of mesopore materials are still observed in Fig. 5A. The pore size distribution is shown in Fig. 5B indicating that over Au/TS-1 catalysts, some small mesopores were created with a shoulder peak of pore size at about 4.1 nm, which was in agreement with the previous study [13,45].

3.3. Propylene epoxidation over the Au/TS-1 catalysts

3.3.1. Influence of IL on the catalytic performance of the Au/TS-1 catalysts

The test results of the 0.5Au/TS-1(35)-IL catalyst through the ILEI method, the 0.5Au/TS-1(35) catalyst without the IL assistance

Table 2
Characterization of the Au/TS-1 catalysts.

Sample	Normal Si/Ti	D_{TS-1} (nm)	S_{BET} ($m^2\ g^{-1}$)	Pore diameter[a] (nm)	Pore vol.[b] ($cm^3\ g^{-1}$)	Actual Au loading (wt.%)
0.25Au/TS-1(35)-IL	35	270 ± 22	409	5.8	0.34	0.25
0.5Au/TS-1(35)-IL	35	270 ± 22	403	6.0	0.34	0.5
1.0Au/TS-1(35)-IL	35	270 ± 22	385	8.5	0.32	1.0
0.5Au/TS-1(48)-IL	48	253 ± 23	410	6.7	0.36	0.5
0.5Au/TS-1(100)-IL	100	244 ± 21	339	4.6	0.21	0.5
0.5Au/TS-1(200)-IL	200	234 ± 26	354	6.8	0.31	0.5

[a] Calculated from the desorption branch of nitrogen isotherm by using the BJH model.
[b] Calculated from the volume adsorbed of P/P_0 at 0.99.

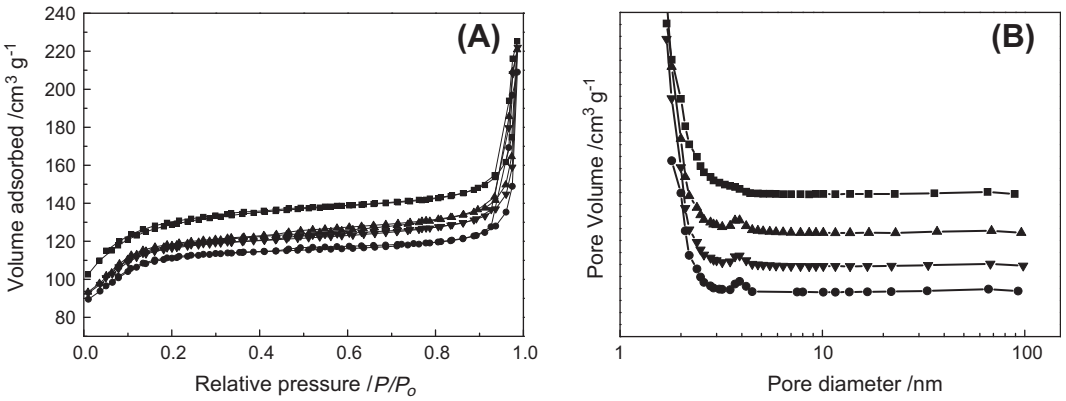

Fig. 5. Nitrogen adsorption–desorption isotherms (A) and the corresponding pore size distributions (B) for different Au loadings; ■: TS-1(35), ▲:0.25Au/TS-1(35)-IL, ▼: 0.5Au/TS-1(35)-IL, ●: 1.0Au/TS-1(35)-IL.

and the 0.5Au/TS-1(35)-pH catalyst through acidifying the colloid solution are presented in Table 3 and Fig. 6. Very low C_3H_6 conversion of 0.8% and H_2 efficiency of 4.9% were obtained with the catalyst 0.5Au/TS-1(35), resulting in a very low PO formation rate of 9.2 $g_{po}\ K\ g_{cat.}^{-1}\ h^{-1}$. The catalyst 0.5Au/TS-1(35)-pH only gave propylene conversion of 5.0 and PO formation rate of 60.4 $g_{po}\ K\ g_{cat.}^{-1}\ h^{-1}$. In contrast, C_3H_6 conversion was markedly enhanced to 10.1% with 0.5Au/TS-1(35)-IL, leading to a high PO formation rate of 120.2 $g_{po}\ K\ g_{cat.}^{-1}\ h^{-1}$. Therefore, the catalytic performance of the Au/TS-1 catalysts could be enhanced by adopting the ILEI method and using IL [BMIM][BF_4].

We are interested in understanding the role of [BMIM][BF_4] in the ILEI method. It is generally recognized that UV–vis spectroscopy could be used to examine the surface plasmon resonance (SPR) of NPs in aqueous suspensions. The UV–vis spectrum of the filtrate of the three catalysts is shown in Fig. 7. The UV–vis spectra (spectrum b and c) of the pale yellow filtrate (photographs d and e) of 0.5Au/TS-1(35)-IL and 0.5Au/TS-1(35)-pH did not show any SPR band at about 540 nm, indicating that GNPs were fully immobilized on the TS-1 support. In contrast, the UV–vis spectrum (spectrum a) for the reddish-pink filtrate (photograph f) of 0.5Au/TS-1(35) clearly exhibited a SPR band at about 540 nm, suggesting that a certain amount of the GNPs remained in the filtrate. The AAS analysis results of the Au concentration in the filtrate showed that only about 70% of gold in the precursor solution was immobilized onto the TS-1. The GNPs could be completely immobilized onto the TS-1 by sulfuric acid and IL; however, the catalytic performance of the catalyst 0.5Au/TS-1(35)-IL was superior to that of the catalyst 0.5Au/TS-1(35)-pH.

NPs are immobilized on support materials by the electrostatic attractive forces between support materials and NPs during the process of the SI method. Usually the colloid solution is acidified, so that its pH value is below the isoelectric point (IEP) of support materials, which results in positive charges on the support surface, attracting the NPs with negative charges. Grunwaldt et al. [21,23] reported the preparation of supported Au catalysts for low-temperature CO oxidation via this method. Hutchings and coworkers [20,22] reported that Au–Pd NPs were supported on TiO_2 and carbon prepared via SI technique for solvent-free oxidation of benzyl alcohol. The real surface of the biosynthesized GNPs was covered by anions that were associated with the negatively charged biomolecules with carboxyl groups, protecting the GNPs from aggregating [37]. The IEP value of the TS-1 support is about 2–3 [50]. Here, the catalyst 0.5Au/TS-1(35)-pH was prepared at the pH value of 2 below the IEP of TS-1 support; the surface of TS-1 support was covered by positive charges, which attract the GNPs. As a consequence, the GNPs can be completely adsorbed on the TS-1 support. The catalyst 0.5Au/TS-1(35) was prepared at the pH value of 3.3 above the IEP of TS-1 support, so the surface of TS-1 support was covered by negative charges, which repulse the GNPs and prevent their adsorption. As a result, the GNPs cannot be completely adsorbed on the TS-1 support. On the contrary, the GNPs can be fully adsorbed on the TS-1(35) support with IL at the same conditions.

In order to further investigate the role of [BMIM][BF_4] in promoting adsorption of the GNPs on the TS-1 support with IL, the zeta potentials (ζ) of the TS-1 supports under different [BMIM][BF_4] concentrations were obtained. ζ characterizes the potential difference between the slipping plane of the solid particles and bulk solution, which could reflect the state of the ions in the electrical double layer [51]. As shown in Fig. 8, the initial ζ of the TS-1(35) support was −35.78 mV, revealing that anions dominated on the surface of the TS-1 support according to the electrical double-layer theory [51]. When a moderate amount of [BMIM][BF_4] was added to the TS-1 hydrosol, the absolute value of the negative ζ decreased, indicating that $[BMIM]^+$ squashed into the stern layer and neutralized part of the negative charges. In such a process, the van der Waals forces as well as the electrostatic attractive forces between $[BMIM]^+$ ions and the negative charges in the stern layer

Table 3
Catalytic performance for propylene epoxidation over Au/TS-1 catalysts.

Au catalysts	Actual Au loading (wt.%)	Conversion of C_3H_6 (%)	Efficiency of H_2 (%)	Selectivity (%)						PO formation rate (g_{po} K $g_{cat.}^{-1}$ h^{-1})
				PO	Et	Pr	An	Ac	CO_2	
0.5Au/TS-1(35)	0.35	0.8	4.9	70.9	8.9	0.0	5.1	10.3	4.7	9.2
0.5Au/TS-1(35)-pH	0.5	5.0	16.9	73.2	8.6	2.0	6.4	7.3	2.5	60.4
0.5Au/TS-1(35)-IL	0.5	10.1	27.6	72.1	10.9	1.5	4.3	8.4	2.7	120.2

Reaction conditions: Catalyst, 0.15 g; temperature, 300 °C; feed gas, $C_3H_6/O_2/H_2/N_2$ = 1/1/1/7(vol.%); space velocity, 7000 mL h^{-1} $g_{cat.}^{-1}$; all the data were taken under a steady state after 2-h duration. Propylene oxide, PO; ethanol, Et; propanol, Pr; acrolein, An; acetone, Ac; pretreated under air at 375 °C for 6 h.

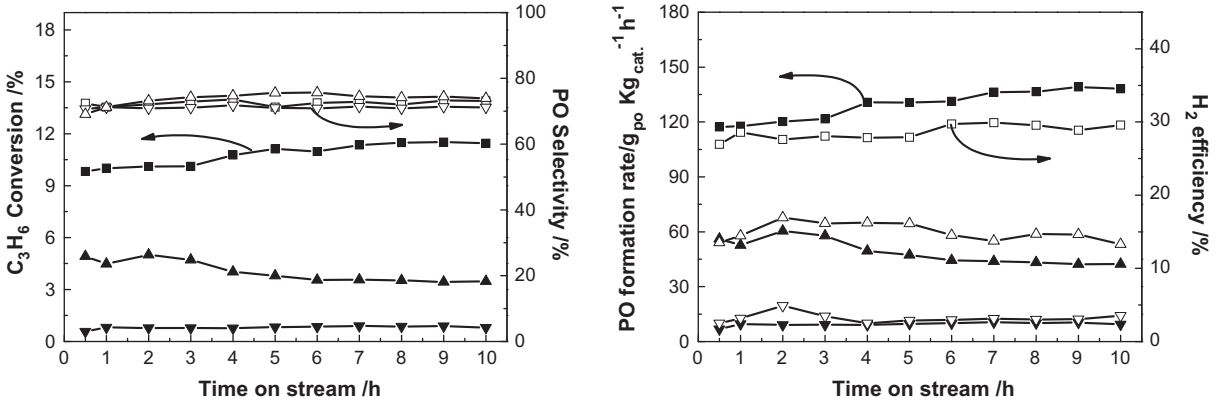

Fig. 6. Epoxidation of propylene over Au/TS-1; ■, □: 0.5Au/TS-1(35)-IL, ▲, △: 0.5Au/TS-1(35)-pH, ▼, ▽: 0.5Au/TS-1(35); reaction conditions: Catalyst, 0.15 g; temperature, 300 °C; feed gas, $C_3H_6/O_2/H_2/N_2$ = 1/1/1/7(vol.%); space velocity, 7000 mL h^{-1} $g_{cat.}^{-1}$.

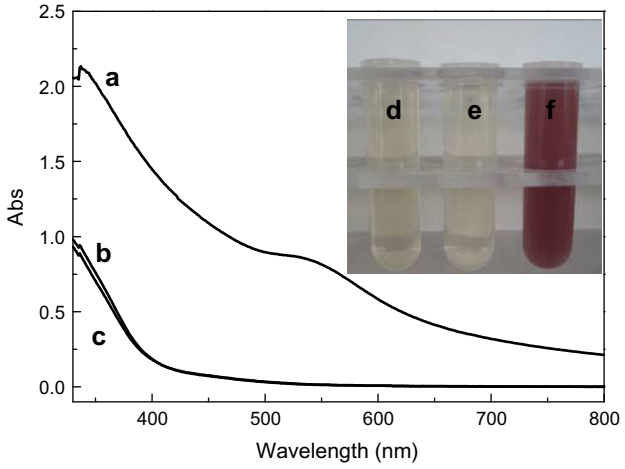

Fig. 7. UV–vis spectra of the filtrate of Au/TS-1 catalysts; (a) 0.5Au/TS-1(35) (photograph f), (b) 0.5Au/TS-1(35)-IL (photograph d), and (c) 0.5Au/TS-1(35)-pH (photograph e).

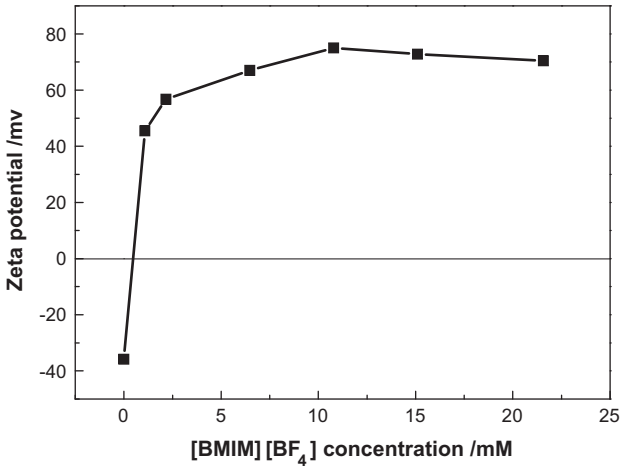

Fig. 8. Zeta potential of the TS-1(35) versus [BMIM][BF_4] concentrations.

played a positive role. When the concentration of [BMIM][BF_4] was 1.1 mM, ζ became positive, suggesting that $[BMIM]^+$ could still enter into the stern layer. In this circumstance, the electrostatic forces between the $[BMIM]^+$ ions inside and outside the stern layer became repulsive and had a negative effect on continual access of the $[BMIM]^+$ ions to the stern layer; However, it is well known that in general the specific adsorption of an ion is enhanced by larger size, which is a function of ion size [51]. Hence, driven by strong van der Waals forces, at this stage, $[BMIM]^+$ ions could still be adsorbed into the stern layer and ζ kept growing when concentration of [BMIM][BF_4] increased from 1.1 to 6.5 mM. For the concentration of [BMIM][BF_4] from 6.5 to 21.6 mM, ζ changed little (Fig. 8), indicating saturated adsorption of $[BMIM]^+$ on the TS-1 support, and a balance was thus established between the van der Waals attractive forces, the electrostatic repulsive forces, and steric hindrance effects. Fig. 9 shows the zeta potential behavior and IEP of TS-1(35) with or without IL in the suspension. The IEP of TS-1(35) with IL had a pH value of 8.0 which was shifted from the pH value of 2.8 for the TS-1(35) because of the special adsorption of $[BMIM]^+$ ions. Therefore, the GNPs with negative charges can be fully adsorbed on the TS-1 support with $[BMIM]^+$ ions. And the interaction between GNPs and TS-1 supports by the ILEI method was stronger than that by acidifying the colloid solution. The enhancement of catalytic performance could be attributed to stronger interaction between GNPs and TS-1 supports caused by IL.

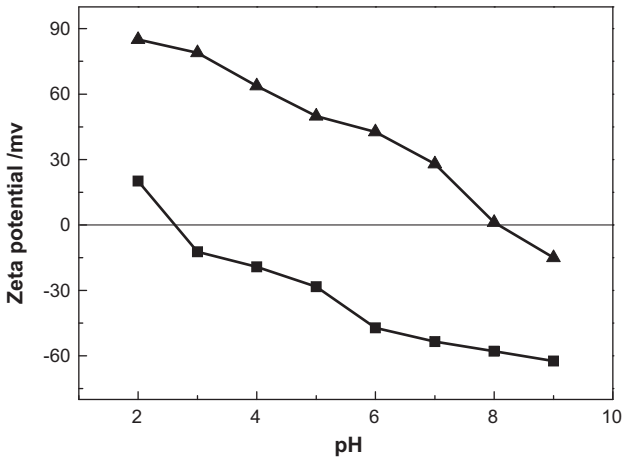

Fig. 9. Zeta potential curves of TS-1(35) (■) and TS-1(35)-IL (▲) versus pH values.

3.3.2. Influence of Au loadings and Si/Ti ratio over the catalytic performance of the Au/TS-1 catalysts

The epoxidation performance of Au/TS-1 catalysts with Au loadings of 0.25–1.0 wt.% at 300 °C was also tested. The catalytic performance of these catalysts is presented in Fig. 10. It can be seen that the catalyst 0.25Au/TS-1(35)-IL with the lowest Au loading of 0.25% gave the propylene conversion of 5.1% and PO formation rate of 60.7 g_{po} K $g_{cat.}^{-1}$ h^{-1}. The catalyst 0.5Au/TS-1(35)-IL with intermediate Au loading gave intermediate propylene conversion and PO selectivity. The catalyst 1.0Au/TS-1(35)-IL with the highest Au loadings of 1.0% gave the highest propylene conversion of 14.6% and PO formation rate of 164.4 g_{po} K $g_{cat.}^{-1}$ h^{-1}, which are the highest in data reported so far. From the above analysis, we can see that the catalytic performance of Au/TS-1 catalysts was strongly affected by Au loading.

Si:Ti ratio is another vital parameter influencing the catalytic performance of Au/TS-1 catalysts. The influence of Si/Ti ratio upon the catalytic performance with the catalysts 0.5Au/TS-1(35)-IL, 0.5Au/TS-1(48)-IL, 0.5Au/TS-1(100)-IL, and 0.5Au/TS-1(200)-IL was studied. The catalytic performance of these catalysts is presented in Fig. 11, indicating that decreasing titanium contents resulted in the increase in PO rate for the catalysts. Moreover, the H_2 efficiency increased from 5.9% to 27.6% with the decrease in Si/Ti ratio from 200 to 35. We also found that the catalysts 0.5Au/TS-1(35)-IL and 0.5Au/TS-1(48)-IL with lower Si/Ti ratio showed high stability and the catalysts 0.5Au/TS-1(100)-IL and 0.5Au/TS-1(200)-IL with higher Si/Ti ratio suffered deactivation.

Uphade et al. [10] proposed that hydrogen peroxide formed from H_2 and O_2 over the gold surface was first converted into a hydroperoxo-like species on the Ti^{4+}–SiO_2 surface, which then reacted with propylene preadsorbed on the support surface to produce PO. The influence of Au loadings and Si/Ti ratio on the catalytic performance of Au/TS-1 catalysts might be explained as follows. The H_2 conversion increased if Au loadings of the catalyst increased. Then, H_2 reacted with O_2 over the surface of GNPs to produce more H_2O_2 and form more Ti–OOH at active Ti^{4+} sites, giving rise to the increase in the propylene conversion. However, the active Ti^{4+} sites were limited, and the effective capture of H_2O_2 by active Ti^{4+} sites to form Ti–OOH became very important for C_3H_6 epoxidation. Otherwise, excessive H_2O_2 will be directly decomposed to produce H_2O and did not contribute to PO synthesis leading to lower H_2 utilization efficiency. Hence, the H_2 utilization efficiency will increase with decreasing Si/Ti ratio according to the analysis above.

3.3.3. Possible reasons for excellent performance of the Au/TS-1 catalysts under high reaction temperature

The reaction temperature is one of the vital parameters that are related to the activation of reactants and the efficiency of hydroperoxide species [52,53]. The catalytic performance of the catalyst 0.5Au/TS-1(48)-IL at 220, 240, 260, 280, and 300 °C is presented in Fig. 12. It can be seen that when the reaction temperature was 220 °C, the conversion of propylene was only 2.7% albeit with H_2 efficiency and medium PO selectivity as high as 54.3% and 81.7%, respectively. When the reaction was conducted at 300 °C, the propylene conversion was promoted to 8.8%, whereas the PO selectivity decreased to 73.8% and H_2 efficiency was 21.0%. Based on the reaction temperature investigations, the Arrhenius plots for the formation of PO, ethanol, and CO_2 gave apparent activation energies of 30, 57, and 51 kJ mol^{-1}, respectively. These activation energy values are close to those reported in literatures [15,16], suggesting that the reactions in our experimental system occur via similar mechanisms.

In the previous studies on propylene epoxidation using gold catalysts [14,16–18,54,55], reaction temperatures were usually less than 200 °C. Above this temperature, the PO selectivity was reported to drop significantly [9,56]. This easily leads to confusions about the high activity and PO selectivity (above 70%) of our catalyst at reaction temperature as high as 300 °C in the presence of H_2 and O_2. As a matter of fact, Haruta et al., who is a well-known authority in the field of propylene epoxidation, have reported high yield of propylene oxide (PO) with its selectivity above 80% using silylated Au catalysts at a temperature of 250 °C, about 100 °C higher than the optimum temperature for non-silylated Au

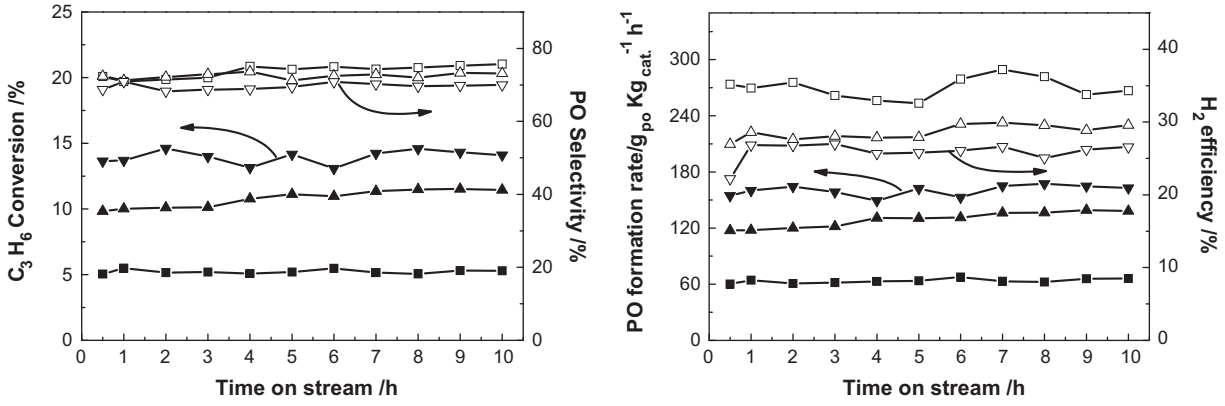

Fig. 10. Epoxidation of propylene over Au/TS-1 with different Au loadings; ■, □: 0.25Au/TS-1(35)-IL, ▲, △: 0.5Au/TS-1(35)-IL, ▼, ▽: 1.0Au/TS-1(35)-IL; reaction conditions: Catalyst, 0.15 g; temperature, 300 °C; feed gas, $C_3H_6/O_2/H_2/N_2$ = 1/1/1/7(vol.%); space velocity, 7000 mL h^{-1} $g_{cat.}^{-1}$.

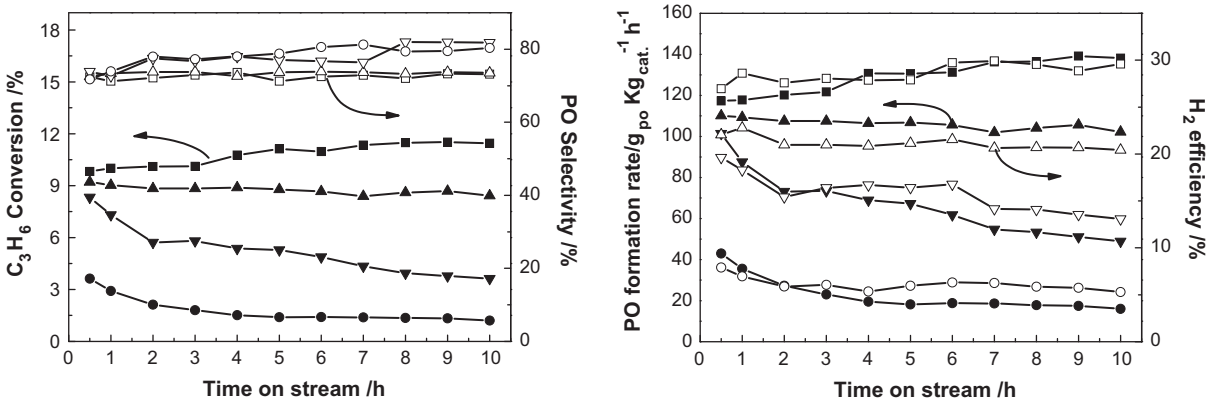

Fig. 11. Epoxidation of propylene over Au/TS-1 with different Si/Ti ratios; ■, □: 0.5Au/TS-1(35), ▲, △: 0.5Au/TS-1(48)-IL, ▼,▽: 0.5Au/TS-1(100)-IL, ●, ○: 0.5Au/TS-1(200)-IL; reaction conditions: Catalyst, 0.15 g; temperature, 300 °C; feed gas, $C_3H_6/O_2/H_2/N_2$ = 1/1/1/7 (vol.%); space velocity, 7000 mL h^{-1} $g_{cat.}^{-1}$.

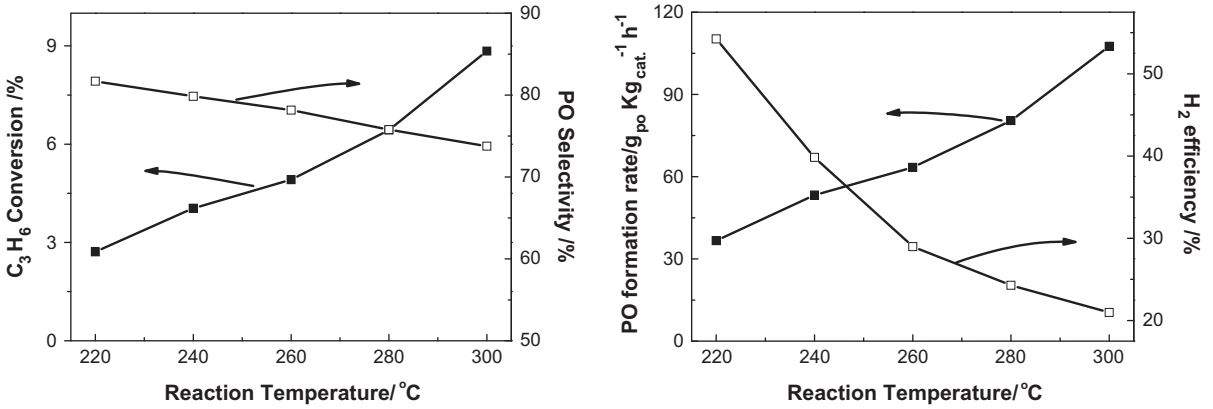

Fig. 12. C_3H_6 conversion, PO selectivity, H_2 efficiency, PO formation rate as a function of reaction temperature over 0.5Au/TS-1(48)-IL; reaction conditions: Catalyst, 0.15 g; feed gas, $C_3H_6/O_2/H_2/N_2$ = 1/1/1/7(vol.%); space velocity, 7000 mL h^{-1} $g_{cat.}^{-1}$.

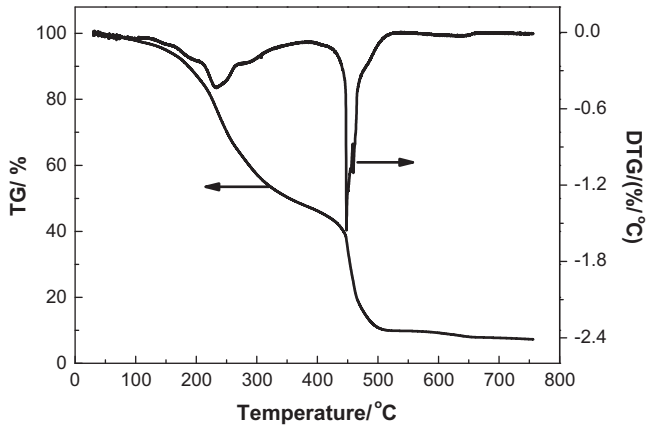

Fig. 13. Simultaneous TG and DTG analysis profiles for the biomass of *C. platycladi* leaf. The biomass was obtained by removing the water of *C. platycladi* extract.

catalysts [57]. It has been speculated that the $SiMe_3$ groups on the catalyst might inhibit the transfer of the active intermediate H_2O_2 from the gold to the Ti sites, thus leading to poor activity at low temperature [57].

Herein, to figure out the possible reasons for the high activity and selectivity of the 0.5Au/TS-1(48)-IL catalyst, TG and differential TG (DTG) analysis of the extract of *C. platycladi* was conducted as shown in Fig. 13. The extract was dried at 50 °C under vacuum for 10 h to obtain the powder plant biomass. It is widely acknowledged that there are a large number of known or unknown complicated biomolecules in *C. platycladi* extract [38,44,45]. According to the TG profile, the main weight loss was between 200 and 500 °C, and the main DTG peaks centering at about 230 and 450 °C. The weight loss at 230 °C was attributed to the loss of some volatile compounds, and the weight loss at 450 °C was due to crack and vaporization of the organic molecules. Therefore, there remains biomolecules on the surface of the Au/TS-1 catalyst after calcination at 375 °C. Such residual biomolecules might be even larger than the $SiMe_3$ groups, leading to larger steric hindrance on the transfer of the active intermediate H_2O_2 from the gold to the Ti sites. This might explain why the optimal reaction temperature in our case was even higher than that of the silylation [57].

Although the reaction temperature is relatively high compared with conventional catalysts, our catalysts are highlighted by their excellent catalytic stability and high selectivity (above 70%) at a relatively high reaction temperature. This might also be attributed to the existence of residual biomolecules on the catalysts which were speculated to play dual roles as both catalyst surface modifier and GNP stabilizer. In the first place, modification of the catalyst by the residual biomolecules, similar to silylation [57], might change the surface property of the support from hydrophilicity to hydrophobicity; the surface acidic sites of the support, which are assumed to be active for ring-opening reactions [58], were also passivated, hence favoring easy desorption of PO from the support and thus inhibiting further oxidation of PO [11,57]. In addition, we also studied the performance of the 0.5Au/TS-1(35)-IL catalyst by bio-reduction with the IL assistance that has high extraframework

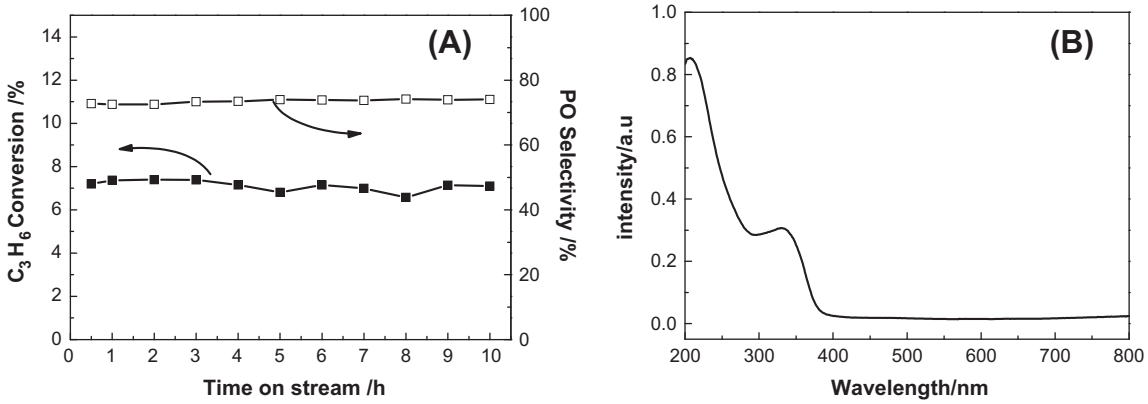

Fig. 14. Epoxidation of propylene over 0.5Au/TS-1(35)-IL catalyst with high extraframework Ti content (A) and UV–vis spectra (B) of TS-1(35); reaction conditions: Catalyst, 0.15 g; temperature, 300 °C; feed gas, $C_3H_6/O_2/H_2/N_2$ = 1/1/1/7(vol.%); space velocity, 7000 mL h^{-1} $g_{cat.}^{-1}$.

Ti content, as illustrated by the DRUV–vis spectroscopy in Fig. 14B. It is generally believed that excess of anatase and extraframework Ti in Au–Ti catalysts could accelerate PO oligomerization, thus blocking the active sites and deactivating the catalyst [59]. Nonetheless, different from the conventionally prepared catalysts [17], the catalyst 0.5Au/TS-1(35)-IL showed high catalytic stability (Fig. 14A). Such a result is consistent with the previous speculation that existence of the residual biomolecules might be able to enhance the desorption of PO from the support, thus dramatically decreasing the chances of PO oligomerization. Also, it has been proved that biomolecules could work as both reductants of the metal precursors and stabilizing agents of GNPs [37,44,45,60]. And compared with the citrate-protected GNPs, biosynthesized GNPs under the protection of unknown biomolecules possess stronger stability toward salt-induced aggregation [60]. Identically, in the 0.5Au/TS-1(35)-IL catalyst, the existence of the residual biomolecules on the surface of GNPs could prevent GNPs from aggregation even at a relatively high temperature [44,45,60]. As evidenced by TEM image (Fig. 3B), the GNPs on the support maintained the same particle size (3.1 nm) without agglomeration after calcination at 375 °C.

Above is a plausible explanation for the excellent activity and high selectivity of the Au/TS-1 catalysts at a relatively high reaction temperature. As a matter of fact, prior to this work, our group has already reported active Au/TS-1 catalysts by bio-reduction method without the addition of ionic liquid for propylene epoxidation with similar selectivity at 300 °C [44,45]. As well, according to Vilchis-Nestor et al., biosynthesized catalysts demonstrated much better activity in oxidation and hydrogenation of CO than the conventionally prepared catalysts at high temperature [43]. Such results, in addition to this work, clearly indicate the undeniable advantages and great potentials of the bio-reduction method in the preparation of precious metal catalysts. Admittedly, due to the complicate composition of the aqueous extract of the plant biomass, the exact roles of the biomolecules in the biosynthesis of catalyst and their catalytic performance remain unknown, and our efforts are directed toward achieving this goal in the nearest future.

4. Conclusion

In summary, we presented an ILEI method to prepare highly stable and active Au/TS-1 nanocatalysts using [BMIM][BF_4] toward propylene epoxidation. In the ILEI method, the IEP of TS-1(35) was shifted from the pH value of 2.6 to 8.0 and the ζ of the TS-1 hydrosol can be changed by cations of [BMIM][BF_4] because of the special adsorption, which results in positive charges on the support surface, attracting the GNPs with negative charges prepared by the biosynthesis using *C. platycladi* extract. Therefore, the GNPs with negative charges can be fully adsorbed on the TS-1 support by the electrostatic attractive forces. And the interaction between GNPs and TS-1 supports by the ILEI method was stronger than that by acidifying the colloid solution. The enhancement of catalytic performance could be attributed to stronger interaction between GNPs and TS-1 supports caused by IL. The excellent activity and high selectivity of the Au/TS-1 catalysts at a relatively high reaction temperature might be attributed to the existence of residual biomolecules on the catalysts. They were supposed to prevent the GNPs from agglomeration and change the surface property of the support, thus promoting desorption of PO from the catalysts. We believe that the ILEI method can be extended to fabrication of other supported noble metal nanocatalysts, and the resulting materials could be used as efficient nanocatalysts.

Acknowledgments

This work was supported by the National Natural Science Foundation of China (Nos. 21036004, 20776120, and 20976146), the Fundamental Research Funds for the Central Universities (No. 2010121051), the Research Fund for the Doctoral Program of Higher Education of China (No. 20100121110032), and the Natural Science Foundation of Fujian Province of China (Grant Nos. 2010J05032, 2010J01052, and 2008J0169). Prof. Mingshu Chen is gratefully acknowledged for his helpful discussion.

References

[1] T.A. Nijhuis, M. Makkee, J.A. Moulijn, B.M. Weckhuysen, Ind. Eng. Chem. Res. 45 (2006) 3447.
[2] M. McCoy, Chem. Eng. News 79 (2001) 19.
[3] M.G. Clerici, G. Bellussi, U. Romano, J. Catal. 129 (1991) 159.
[4] M.G. Clerici, P. Lngallina, J. Catal. 140 (1993) 71.
[5] J.M. Campos-Martin, G. Blanco-Brieva, J.L.G. Fierro, Angew. Chem. Int. Ed. 45 (2006) 6962.
[6] T. Hayashi, K. Tanaka, M. Haruta, J. Catal. 178 (1998) 566.
[7] C. Qi, M. Okumura, T. Akita, M. Haruta, Appl. Catal. A – Gen. 263 (2004) 19.
[8] B.S. Uphade, Y. Yamada, T. Akita, T. Nakamura, M. Haruta, Appl. Catal. A – Gen. 215 (2001) 137.
[9] A.K. Sinha, S. Seelan, T. Akita, S. Tsubota, M. Haruta, Appl. Catal. A – Gen. 240 (2003) 243.
[10] B.S. Uphade, T. Akita, T. Nakamura, M. Haruta, J. Catal. 209 (2002) 331.
[11] A.K. Sinha, S. Seelan, M. Okumura, T. Akita, S. Tsubota, M. Haruta, J. Phys. Chem. B 109 (2005) 3956.
[12] A.K. Sinha, S. Seelan, S. Tsubota, M. Haruta, Angew. Chem. Int. Ed. 43 (2004) 1546.
[13] H.W. Yang, D.L. Tang, X.N. Lu, Y.Z. Yuan, J. Phys. Chem. C 113 (2009) 8186.
[14] J.Q. Lu, X.M. Zhang, J.J. Bravo-Suarez, T. Fujitani, S.T. Oyama, Catal. Today 147 (2009) 186.
[15] L. Cumaranatunge, W.N. Delgass, J. Catal. 232 (2005) 38.
[16] B. Taylor, J. Lauterbach, W.N. Delgass, Catal. Today 123 (2007) 50.

[17] N. Yap, R.P. Andres, W.N. Delgass, J. Catal. 226 (2004) 156.
[18] B. Taylor, J. Lauterbach, W.N. Delgass, Appl. Catal. A – Gen. 291 (2005) 188.
[19] D.H. Wells, W.N. Delgass, K.T. Thomson, J. Am. Chem. Soc. 126 (2004) 2956.
[20] N. Dimitratos, J.A. Lopez-Sanchez, D. Morgan, A.F. Carley, R. Tiruvalam, C.J. Kiely, D. Bethell, G.J. Hutchings, Phys. Chem. Chem. Phys. 11 (2009) 5142.
[21] J.D. Grunwaldt, C. Kiener, C. Wogerbauer, A. Baiker, J. Catal. 181 (1999) 223.
[22] J.A. Lopez-Sanchez, N. Dimitratos, P. Miedziak, E. Ntainjua, J.K. Edwards, D. Morgan, A.F. Carley, R. Tiruvalam, C.J. Kiely, G.J. Hutchings, Phys. Chem. Chem. Phys. 10 (2008) 1921.
[23] J.D. Grunwaldt, M. Maciejewski, O.S. Becker, P. Fabrizioli, A. Baiker, J. Catal. 186 (1999) 458.
[24] J. Chou, E.W. McFarland, Chem. Commun. (2004) 1648.
[25] J. Huang, T. Jiang, B.X. Han, H.X. Gao, Y.H. Chang, G.Y. Zhao, W.Z. Wu, Chem. Commun. (2003) 1654.
[26] J. Dupont, R.F. de Souza, P.A.Z. Suarez, Chem. Rev. 102 (2002) 3667.
[27] J. Dupont, G.S. Fonseca, A.P. Umpierre, P.F.P. Fichtner, S.R. Teixeira, J. Am. Chem. Soc. 124 (2002) 4228.
[28] K.S. Kim, D. Demberelnyamba, H. Lee, Langmuir 20 (2004) 556.
[29] J. Huang, T. Jiang, H.X. Gao, B.X. Han, Z.M. Liu, W.Z. Wu, Y.H. Chang, G.Y. Zhao, Angew. Chem. Int. Ed. 43 (2004) 1397.
[30] S.D. Miao, Z.M. Liu, B.X. Han, J. Huang, Z.Y. Sun, J.L. Zhang, T. Jiang, Angew. Chem. Int. Ed. 45 (2006) 266.
[31] X.M. Ma, Y.X. Zhou, J.C. Zhang, A.L. Zhu, T. Jiang, B.X. Han, Green Chem. 10 (2008) 59.
[32] J.L. Gardea-Torresdey, K.J. Tiemann, G. Gamez, K. Dokken, S. Tehuacanero, M. José-Yacamán, J. Nanopart. Res. 1 (1999) 397.
[33] S.S. Shankar, A. Rai, B. Ankamwar, A. Singh, A. Ahmad, M. Sastry, Nat. Mater. 3 (2004) 482.
[34] S.S. Shankar, A. Ahmad, R. Pasricha, M. Sastry, J. Mater. Chem. 13 (2003) 1822.
[35] S.P. Chandran, M. Chaudhary, R. Pasricha, A. Ahmad, M. Sastry, Biotechnol. Prog. 22 (2006) 577.
[36] S.S. Shankar, A. Rai, A. Ahmad, M. Sastry, J. Colloid Interf. Sci. 275 (2004) 496.
[37] J.L. Huang, Q.B. Li, D.H. Sun, Y.H. Lu, Y.B. Su, X. Yang, H.X. Wang, Y.P. Wang, W.Y. Shao, N. He, J.Q. Hong, C.X. Chen, Nanotechnology 18 (2007) 105104.
[38] Y. Zhou, W.S. Lin, J.L. Huang, W.T. Wang, Y.X. Gao, L.Q. Lin, Q.B. Li, L. Lin, M.M. Du, Nanoscale Res. Lett. 5 (2010) 1351.
[39] X. Yang, Q.B. Li, H.X. Wang, J.L. Huang, L.Q. Lin, W.T. Wang, D.H. Sun, Y.B. Su, J.B. Opiyo, L.W. Hong, Y.P. Wang, N. He, L.S. Jia, J. Nanopart. Res. 12 (2010) 1589.
[40] L.Q. Lin, W.T. Wang, J.L. Huang, Q.B. Li, D.H. Sun, X. Yang, H.X. Wang, N. He, Y.P. Wang, Chem. Eng. J. 162 (2010) 852.
[41] L.S. Jia, Q. Zhang, Q.B. Li, H. Song, Nanotechnology 20 (2009) 385601.
[42] J.L. Huang, W.T. Wang, L.Q. Lin, Q.B. Li, W.S. Lin, M. Li, S. Mann, Chem. – Asian J. 4 (2009) 1050.
[43] A.R. Vilchis-Nestor, M. Avalos-Borja, S.A. Gomez, J.A. Hernandez, A. Olivas, T.A. Zepeda, Appl. Catal. B – Environ. 90 (2009) 64.
[44] G.W. Zhan, M.M. Du, J.L. Huang, Q.B. Li, Catal. Commun. 12 (2011) 830.
[45] G.W. Zhan, M.M. Du, D.H. Sun, J.L. Huang, X. Yang, Y. Ma, A.R. Ibrahim, Q.B. Li, Ind. Eng. Chem. Res. 50 (2011) 9019.
[46] R.B. Khomane, B.D. Kulkarni, A. Paraskar, S.R. Sainkar, Mater. Chem. Phys. 76 (2002) 99.
[47] T. Armaroli, F. Milella, B. Notari, R.J. Willey, G. Busca, Top Catal. 15 (2001) 63.
[48] E. Duprey, P. Beaunier, M.A. SpringuelHuet, E. BozonVerduraz, J. Fraissard, J.M. Manoli, J.M. Bregeault, J. Catal. 165 (1997) 22.
[49] E.R. Talaty, S. Raja, V.J. Storhaug, A. Dolle, W.R. Carper, J. Phys. Chem. B 108 (2004) 13177.
[50] J.W. Lee, S. Kong, W.S. Kim, J. Kim, Mater. Chem. Phys. 106 (2007) 39.
[51] A.W. Adamson, A.P. Gast, John Wiley and Sons, Inc., New York, 1997 (Chapter 5).
[52] W. Laufer, R. Meiers, W. Holderich, J. Mol. Catal. A – Chem. 141 (1999) 215.
[53] L.Y. Chen, G.K. Chuah, S. Jaenicke, J. Mol. Catal. A – Chem. 132 (1998) 281.
[54] J.H. Huang, E. Lima, T. Akita, A. Guzman, C.X. Qi, T. Takei, M. Haruta, J. Catal. 278 (2011) 8.
[55] J.H. Huang, T. Takei, T. Akita, H. Ohashi, M. Haruta, Appl. Catal. B – Environ. 95 (2010) 430.
[56] B.S. Uphade, S. Tsubota, T. Hayashi, M. Haruta, Chem. Lett. (1998) 1277.
[57] C.X. Qi, T. Akita, M. Okumura, K. Kuraoka, M. Haruta, Appl. Catal. A – Gen. 253 (2003) 75.
[58] M.L. Pena, V. Dellarocca, F. Rey, A. Corma, S. Coluccia, L. Marchese, Microporous Mesoporous Mater. 44 (2001) 345.
[59] G. Mul, A. Zwijnenburg, B. van der Linden, M. Makkee, J.A. Moulijn, J. Catal. 201 (2001) 128.
[60] Y. Zhou, W.S. Lin, H.X. Wang, Q.B. Li, J.L. Huang, M.M. Du, L.Q. Lin, Y.X. Gao, L. Lin, N. He, Langmuir 27 (2011) 166.